

Characterization of degeneration process in combustion instability based on dynamical systems theory

Hiroshi Gotoda,^{1,2,*} Yuta Okuno,² Kenta Hayashi,² and Shigeru Tachibana^{3,†}

¹*Department of Mechanical Engineering, Tokyo University of Science, 6-3-1 Nijjuku, Katsushika-ku, Tokyo 125-0051, Japan*

²*Department of Mechanical Engineering, Ritsumeikan University, 1-1-1 Nojihigashi, Kusatsu-shi, Shiga 525-8577, Japan*

³*Institute of Aeronautical Technology, Japan Aerospace Exploration Agency, 7-44-1 Jindaiji-Higashi, Chofu, Tokyo 182-8522, Japan*

(Received 25 September 2014; published 6 November 2015)

We present a detailed study on the characterization of the degeneration process in combustion instability based on dynamical systems theory. We deal with combustion instability in a lean premixed-type gas-turbine model combustor, one of the fundamentally and practically important combustion systems. The dynamic behavior of combustion instability in close proximity to lean blowout is dominated by a stochastic process and transits to periodic oscillations created by thermoacoustic combustion oscillations via chaos with increasing equivalence ratio [Chaos **21**, 013124 (2011); Chaos **22**, 043128 (2012)]. Thermoacoustic combustion oscillations degenerate with a further increase in the equivalence ratio, and the dynamic behavior leads to chaotic fluctuations via quasiperiodic oscillations. The concept of dynamical systems theory presented here allows us to clarify the nonlinear characteristics hidden in complex combustion dynamics.

DOI: [10.1103/PhysRevE.92.052906](https://doi.org/10.1103/PhysRevE.92.052906)

PACS number(s): 05.45.Tp, 47.70.Pq

I. INTRODUCTION

Nonlinear dynamics of self-excited oscillations, known as thermoacoustic instability, is the result of the closed-loop interaction between unsteady pressure and heat-release rate fluctuations and has become of significant interest in a broad range of areas from combustion to thermal fluid physics [1–8]. The concept of thermoacoustic instability has recently been introduced to the area of applied physics as a means of developing new internal engine systems [5–8]. Lean premixed combustion is known to be an effective method for curtailing nitrogen oxide (NOx) emission from gas-turbine engines of various sizes without impairing combustion efficiency [9]. However, it is notorious for being affected by combustion-driven thermoacoustic instability, referred as to thermoacoustic combustion oscillations, and by other problematic limiting phenomena such as lean blowout and flame flashback. The interaction between the combustion process and the acoustic field in a confined combustion system gives rise to a rich variety of highly nonlinear dynamic behavior of thermoacoustic combustion oscillations, leading to considerable damage in practical and indispensable combustors, affecting aircraft propulsion and land-based gas-turbine engine performance. Numerous experimental and numerical studies have examined the physical excitation mechanisms of thermoacoustic combustion oscillations both with and without swirling flow [10–16]. For instance, as an important physical mechanism associated with the flame-acoustic interaction, it has been proposed by Lawn and Polifke [13] that the significant perturbations in the equivalence ratio, flame front kinematics, turbulence intensity, and length scale generated by acoustic velocity fluctuations result in unsteady heat release rate fluctuations in a swirl-stabilized premixed combustor. A recent review article [17] and a book [18] provide an encompassing overview of the physical mechanism responsible for

thermoacoustic combustion oscillations in various types of laboratory-scale gas turbine combustor.

Nonlinear time series analysis based on dynamical systems theory enables an encompassing and systematic treatment of random-like aperiodic dynamics in nonlinear systems arising in a wide range of disciplines [19–21]. It enables the quantification of many important physical invariants responsible for fractal structure and orbital instability in a system; for example, fractal dimension and Lyapunov exponents, including several types of entropy that can be used to evaluate the complexity itself. In fact, with emphasis being placed on whether or not chaotic and quasiperiodic behavior exists in combustion dynamics, nonlinear time series analysis has been successfully exploited in a broad range of combustion systems, including a thermal pulse combustor [22–24], a ducted premixed combustor [25–27], a gas-turbine model combustor [28], a cellular flame [29], a swirling flame [30], a diffusion flame exposed to acoustic forcing [31], and a diffusion flame with radiative heat loss [32], focusing on the estimation of well-accepted physical invariants such as the correlation dimension [33] and the largest Lyapunov exponent [34,35]. Nowadays, two-dimensional representations for extracting the order and disorder pattern structure in a system, referred to as recurrence plots [36], are frequently applied to the case of an unstable combustion state intermittently switching between thermoacoustic combustion oscillations and small bursts in amplitude [37,38]. We have also conducted systematic studies on nonlinear dynamics of combustion instability in a lean premixed gas-turbine model combustor under a preheated premixture condition [39,40] using different types of nonlinear time series analysis. These include the translation error, referred to as the Wayland method [41], to quantify the degree of parallelism of neighboring trajectories in a constructed phase space, the permutation entropy [42] to evaluate the degree of randomness estimated from a sequence of rank order patterns in the values of temporal evolutions, and multifractal analysis [43] to capture various self-similar structures in terms of a singular spectrum. Chaotic fluctuations generally

*gotoda@rs.tus.ac.jp

†tachibana.shigeru@jaxa.jp

possess short-term predictability and long-term unpredictability characteristics as a consequence of the strong dependence on the initial conditions. Therefore, given a temporal evolution that describes a physical quantity in a system, nonlinear forecasting based on dynamical systems theory can quantify the degree of complexity in the underlying dynamics as well as the fractal dimension, Lyapunov exponents, and entropies, providing a useful index for treating the corresponding dynamical structures of the system. The results obtained [39,40] by nonlinear time series analysis including nonlinear forecasting suggest that the dynamic behavior of combustion instability in close proximity to lean blowout is dominated by a stochastic process associated with fractional Brownian motion and transits to periodic oscillations created by thermoacoustic combustion oscillations via chaos with increasing equivalence ratio. However, in previous studies [39,40], the degeneration of dynamics in thermoacoustic combustion oscillations with a further increase in the equivalence ratio was not explored.

The purpose of this study is to reveal how the combustion dynamics during the degeneration process in a lean premixed gas-turbine model combustor changes with increasing equivalence ratio by using a variety of nonlinear time series analysis methods based on dynamical systems theory that are usually not employed in traditional combustion physics. Our previous study [44] has shown that color recurrence plots enable us to extract ordered and disordered pattern structures in a constructed phase space as two-dimensional representations. We thereby use it in this study to characterize the significant changes in combustion dynamics during the degeneration process. The distinction between deterministic and stochastic processes is an intriguing challenge in nonlinear time series analysis [45–48]. On the basis of our current study on a spatially extended system [49], the nonlinear forecasting methodology, which involves the update of library data in phase space, has been shown to ensure satisfactory performance in distinguishing between a deterministic process and a stochastic process and has been successfully adopted to reveal the possible presence of low-dimensional deterministic chaos in intermittent combustion oscillations [44]. This study also uses the nonlinear forecasting methodology, and we perform a new quantification of the short-term predictability and long-term unpredictability characteristics for the degeneration process. In connection with the sensitive dependence on initial conditions, we also estimate the maximal Lyapunov exponent in combination with a resampling method [50–52] to show the possible presence of chaos. The multiscale entropy based on the application of the sample entropy proposed by Richman and Moorman [53], involving a coarse-graining approach, allows the degree of complexity in dynamical behavior at a multiple temporal scale to be evaluated in terms of the scaling factor. This concept was proposed by Costa *et al.* [54] and has recently been adopted in a wide spectrum of areas in medical physics. We utilize the multiscale entropy method to obtain a more comprehensive interpretation of the complexity in combustion dynamics. This paper is organized as follows: Our experimental system and method are described in Sec. II. In Sec. III, the mathematical framework of nonlinear time series analysis is described. We present and discuss the results in Sec. IV and concluding remarks are provided in Sec. V.

II. EXPERIMENTAL APPARATUS AND METHOD

The lean premixed gas-turbine model combustor employed in this work is identical to that used in our previous study [55]. It comprises five main parts: a blower, an electric heater, an axial swirler, a combustion chamber with a length of 630 mm and a $100 \times 100 \text{ mm}^2$ cross section, and a water-cooled stainless-steel duct. The inlet air is preheated to 700 K and supplied to the combustion chamber at a mass flow rate of 78 g/s. Methane is injected through multiple orifices set 260 mm upstream from the inlet of the combustion chamber as the main fuel. The swirler, which has a vane angle of 45 deg relative to the inlet premixture stream, has the function of a flame holder in this study. A pressure transducer (Kulite Semiconductor Products, Model XTEL-190-15G), which is placed on the wall of the combustion chamber, is used to acquire the pressure fluctuations p inside the combustor. The pressure fluctuations are considered to be an important physical quantity that represents the nonlinear dynamics of the combustion state. The pressure transducer is set 10 mm downstream from the inlet of the combustion chamber since a pronounced effect of thermoacoustic coupling appears in the temporal evolution of the pressure fluctuations. Nonlinear time series analysis is adopted for the temporal evolution of p at a sampling frequency of 25.6 kHz. In this study, we consider equivalence ratios of the methane-air premixture ϕ from 0.52 to 0.6 with the aim of investigating the degeneration process of combustion instability (see Fig. 1). Similarly to in previous work [39,40], we do not adopt active control with secondary fuel injection for the current experimental system so that we can focus on the characterization of the combustion dynamics from the viewpoint of dynamical systems theory.

III. MATHEMATICAL FRAMEWORK OF NONLINEAR TIME SERIES ANALYSIS BASED ON DYNAMICAL SYSTEMS THEORY

We employ nonlinear time series analysis involving the maximal Lyapunov exponent, color recurrence plots, a local predictor, and multiscale entropy. The central idea behind the mathematics of nonlinear time series analysis is described in the following sections. We used MATLAB to develop all the computational codes to obtain them. Note that in this study, the pressure fluctuations p are replaced by x .

A. Maximal Lyapunov exponent

The maximal Lyapunov exponent is an important measure of how nearby orbits in a phase space exponentially diverge with time and allows us to discuss the possible presence of chaos. We adopt the algorithm of Rosenstein *et al.* [34], which is widely recognized as one of the standard and proven methods for evaluating the maximum Lyapunov exponent λ . λ is related to the distance d_k between a reference vector \mathbf{x}_i and its nearest neighbor vectors \mathbf{x}_k as follows:

$$d_k = C_0 e^{\lambda(T_i \Delta t)}, \quad (1)$$

where T_i is the time step, Δt is the sampling period of x , and C_0 is the initial Euclidean distance. The position vectors \mathbf{x} in the phase space are obtained by the embedding theorem [56] and are expressed as $\mathbf{x}(t) = (x(t), x(t + \tau), \dots, x(t + [D - 1]\tau))$,

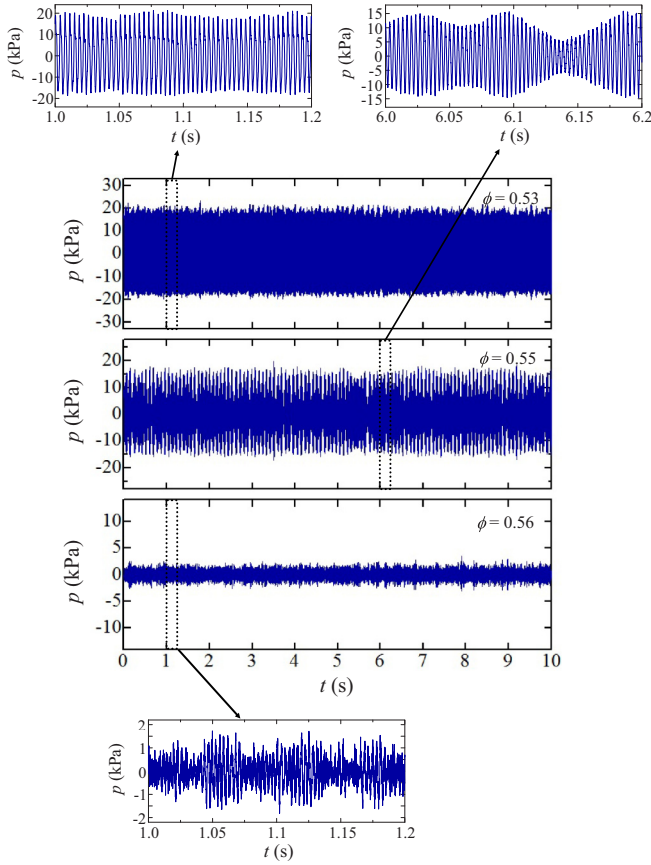


FIG. 1. (Color online) Time variation in p for different equivalence ratios ϕ . Thermoacoustic combustion oscillations at $\phi = 0.53$ significantly degenerate with increasing equivalence ratio.

where τ is the delay time of the D -dimensional phase space. We estimate λ as the gradient of the linear part of the average value $\langle \ln d_k \rangle$ over all values of k plotted against $T_i \Delta t$.

The false nearest neighbors method proposed by Kennel *et al.* [57] is in widespread use for estimating D . Our preliminary test in accordance with the prescription of Kennel *et al.* [57] shows that the phase space for this study can be reconstructed when $D \geq 4$. However, as pointed out by Giannerini and Rosa [51], it does not always allow an appropriate reconstruction to be obtained. Therefore, we vary D from 2 to 10 in this study. Mutual information is a well-known quantity for estimating the optimum time lag of a phase space and has the advantage that one can take into account the nonlinear correlation between the coordinates of the phase space [20], but it does not always give a suitable time lag [51]. In our preliminary test, we vary τ from 3.9×10^{-5} to 1.1×10^{-3} s, and a notable slope of $\langle \ln d_k \rangle$ against $T_s \Delta t$ is obtained for $\tau = 1.1 \times 10^{-4}$ s. Its value corresponds to the time lag at which the mutual information first reaches a minimum [58].

We estimate the maximal Lyapunov exponent λ , but without considering statistical tests, the estimated λ gives a misleading interpretation due to the presence of a dynamic random component in the time series [51]. To assign a rigorous confidence interval in a statistical sense, a resampling method has been proposed by Giannerini and Rosa [50]. As in previous

studies [50–52], we adopt it for the estimation of λ . This method consists of the following four procedures: (i) A new sampling rate of x , namely δt , is made by dividing Δt by the factor f . Note that, in accordance with the prescription of Giannerini and Rosa [50], we set f to 6 in this study. (ii) A point l_1 in the interval $[0, \Delta t]$ is randomly chosen from the time series. (iii) A new replicated time series $y_{1-\delta t}, y_{2-\delta t}, \dots, y_{m-\delta t}$ at the points $l_1, l_2 (= l_1 + \delta t), \dots, l_m (= l_{m-1} + \delta t)$ is obtained by interpolating the time series of x . (iv) After repeating steps (ii) and (iii) for Q sets, Q resampled time series y_1, y_2, \dots, y_Q are finally obtained. We compute λ for all the resampled time series data and statistically investigate its nature. Following previous studies [59,60] on the bootstrap test, we set Q to 1000 in this study.

B. Recurrence plots

It is well recognized that the recurrence plots (RPs) originally proposed by Eckmann *et al.* [36], which are two-dimensional representations consisting of black and white dots, are feasible for extracting ordered and disordered pattern structures in a phase space. This method was first applied to thermoacoustic combustion oscillations in a ducted laminar premixed flame [37] and subsequently to a bluff-body type turbulent combustor [38]. We use a color-coded version of RPs with 256 gradations represented by Eq. (2) instead of the binary version [36], because the color RPs do not require the determination of a threshold value for displaying the black and white dots:

$$\mathbf{R}_{i,j} = \frac{\|\mathbf{x}_i - \mathbf{x}_j\| - \|\mathbf{x}_i - \mathbf{x}_j\|_{\min}}{\|\mathbf{x}_i - \mathbf{x}_j\|_{\max} - \|\mathbf{x}_i - \mathbf{x}_j\|_{\min}}. \quad (2)$$

Here, $\mathbf{R}_{i,j}$ is represented as a color code and begins to exhibit regularly arrayed structures as the periodicity of the dynamics dominates in the phase space.

C. Local predictor

As reported in our recent study [44] on a laboratory-scale gas-turbine model combustor under a nonpreheated premixture condition, chaotic dynamics is highly sensitive to the initial conditions, leading to exponential decay of the prediction time with short-term predictability and long-term unpredictability of the orbits in phase space. On the basis of this important feature, as the nonlinear forecasting methodology in this study, we incorporate the extended version of the Sugihara–May (SM) algorithm [45] as a local nonlinear predictor, which was proposed by Gotoda *et al.* [49] using a spatially extended system. It considers updating the information on the trajectories in the phase space constructed from library data. The temporal evolution of x for $t \in [0; T_f]$ is divided into two intervals, namely, $t \in [0; t_L]$ and $t \in (t_L; T_f]$. These intervals correspond to the library data and test set, respectively. We use the library data to predict the temporal evolution of x . We then make a comparison between x for $t > t_L$ and the corresponding test set. Note that, similarly to in our recent study [49], we construct position vectors in the D -dimensional phase space consisting of $\mathbf{x}(t) = (x(t), x(t - \tau), \dots, x(t - [D - 1]\tau))$. We define $\mathbf{x}_f \equiv \mathbf{x}(t_f)$ as the final point of a trajectory in phase space and search for the nearby vectors \mathbf{x}_k from all the position vectors in the phase space. We denote the predicted value corresponding to \mathbf{x}_k after

T as $x(t_k + T)$. Here, $T = T_s \Delta t$, where T_s is the time step in the future. $\hat{x}(t_f + T)$ is then obtained from \mathbf{x}_f by using the nonlinearly weighted sum of the library data $x(t_k + T)$ as follows:

$$\hat{x}(t_f + T) = \frac{\sum_{k=1}^K \exp(-d_k)x(t_k + T)}{\sum_{k=1}^K \exp(-d_k)}, \quad (3)$$

where $d_k = \|\mathbf{x}(t_f) - \mathbf{x}(t_k)\|$. The predicted $\hat{x}(t_f + T)$ and the test $x(t_k + T)$ are compared by estimating the correlation coefficient defined as

$$C = \frac{\mathbb{E}[x\hat{x}]}{\sigma_x \sigma_{\hat{x}}}, \quad (4)$$

where $\mathbb{E}[x\hat{x}]$ is the covariance between the measured and predicted pressure fluctuations, and σ_x and $\sigma_{\hat{x}}$ are the standard deviations of x and \hat{x} , respectively. When using this nonlinear forecasting methodology, the temporal evolution of x is predicted by updating the library data in the phase space while keeping the size of the updated library data constant. The relation between the correlation coefficient C and the predicted time t_p enables us to extract the short-term predictability and long-term unpredictability characteristics of the dynamics [49]. An important point of the methodology is that if the stochastic process is dominant in the observed dynamics, the incremental process does not exhibit short-term unpredictability; C for the incremental process is low regardless of t_p , which allows us to give a reasonable indicator to distinguish between deterministic and stochastic processes. Note that, in a preliminary test, the distribution of C in terms of t_p remained nearly unchanged within the range of t_L from 2 to 6 s. Therefore, we set t_L to 5 s to ensure a sufficient amount of library data.

D. Multiscale entropy

Entropy can characterize the rate of creation of information owing to the sensitive dependence on initial conditions in chaotic systems, and the most basic kind of entropy is metric entropy, referred to as Kolmogorov–Sinai entropy. Correlation entropy, which corresponds to the lower bound of the Kolmogorov–Sinai entropy, was proposed by Grassberger and Procaccia [33]. It is analogous to the correlation dimension and can be easily computed. However, it is inadequate for estimating the entropy for a finite length of time series data contaminated with noise. To overcome this problem, the approximate entropy [61] and a modified version, sample entropy [53] in analogy with the definition of the correlation entropy, have been proposed as effective approaches to extract the degree of randomness. The latter approximates the Rényi entropy of order two. The mathematical background and physical meaning of the sample entropy were given by Costa *et al.* [62]. They clearly showed that the dynamics of a correlated random process such as colored noise are more complex than those of white noise by taking multiple timescales based on a coarse-graining approach into account in the sample entropy, which yields a better understanding of the randomness than the conventional entropies based on a single scale. On this basis, we apply a multiscale entropy, i.e., the sample entropy, for each coarse-grained time series datum as a function of the scale factor. The multiscale entropy method comprises two procedures: construction of the coarse-grained temporal evolution of x with a scaling factor s' , as shown

in Eq. (5), and estimation of the sample entropy for each coarse-grained temporal evolution in $q_j^{(s')}$ as shown in Eqs. (6) and (7):

$$q_j^{(s')} = \frac{1}{s'} \sum_{t_i=(j-1)s'+1}^{js'} x(t_i), \quad 1 \leq j \leq N/s', \quad (5)$$

$$S_E = \ln \frac{\sum_{i=1}^{N-D} \Theta_i^D}{\sum_{i=1}^{N-D} \Theta_i^{D+1}}, \quad (6)$$

$$\Theta = \begin{cases} 1, & \|\mathbf{q}^D(t_i) - \mathbf{q}^D(t_j)\|_{\max} \leq r \\ 0, & \|\mathbf{q}^D(t_i) - \mathbf{q}^D(t_j)\|_{\max} > r. \end{cases} \quad (7)$$

Here, Θ is the Heaviside function, $\|\mathbf{q}^D(t_i) - \mathbf{q}^D(t_j)\|_{\max}$ is the maximum distance between vectors $\mathbf{q}^D(t_i)$ and $\mathbf{q}^D(t_j)$ in the D -dimensional phase space consisting of $\mathbf{q}^D(t) = (q^{(s')}(t), q^{(s')}(t + \tau), \dots, q^{(s')}(t + [D - 1]\tau))$, and r is the percentage of the time series data lying within one standard deviation of x . A detailed discussion of selecting the optimal value of r was given by Costa *et al.* [62]. They estimated the discrepancies between multiscale entropies for $1/f$ -type colored and white noise as a function of r . The discrepancies for both cases were less than 1% at $r = 0.15$. On this basis, we set r to 0.15 in this study. The multiscale entropy S_E at a low (high) scaling factor represents the degree of complexity in the high (low)-frequency regime in the temporal evolution of x .

IV. RESULTS AND DISCUSSION

Figure 2 depicts the three-dimensional phase space ($x(t), x(t + \tau), x(t + 2\tau)$) for different equivalence ratios ϕ . Thermoacoustic combustion oscillations with large peak-to-peak amplitudes of p at $\phi = 0.53$ (see Fig. 1) exhibit a limit cycle with a relatively large width of periodic orbits. At a higher equivalence ratio of $\phi = 0.55$, we observe the emergence of a torus-like structure with an increased width of the orbits. Both the periodicity and the peak-to-peak amplitude of p (see Fig. 1) are significantly diminished at $\phi = 0.56$, leading to the degeneration of thermoacoustic combustion oscillations. The attractor size decreases, and thereby the orbits converge on the core of the attractor. Tachibana *et al.* [55] showed that the two predominant flames inside their combustor, an *inverted-conical flame* and a *rim flame*, play an essential role in the retention of thermoacoustic combustion oscillations. The former flame is sustained by an inner vortex breakdown zone generated by the swirling flow, while the latter flame is sustained by an outer recirculation zone located in the dump plate. The large fluctuations of the rim flame in particular lead to strong combustion oscillations. At $\phi \geq 0.56$, the large fluctuations cease owing to the changes in the temporal and spatial distributions in the heat release rate. This results in the degeneration of thermoacoustic combustion oscillations. Degeneration owing to an increase in the equivalence ratio has also been observed both in a lean premixed swirl-stabilized combustor under preheated premixture conditions [63] and in our preliminary test using a laboratory-scale gas-turbine model combustor [44] under conditions of a sufficiently high equivalence ratio and a nonpreheated premixture. The present study focuses on the characterization of the degeneration process using nonlinear time series analysis. The probability

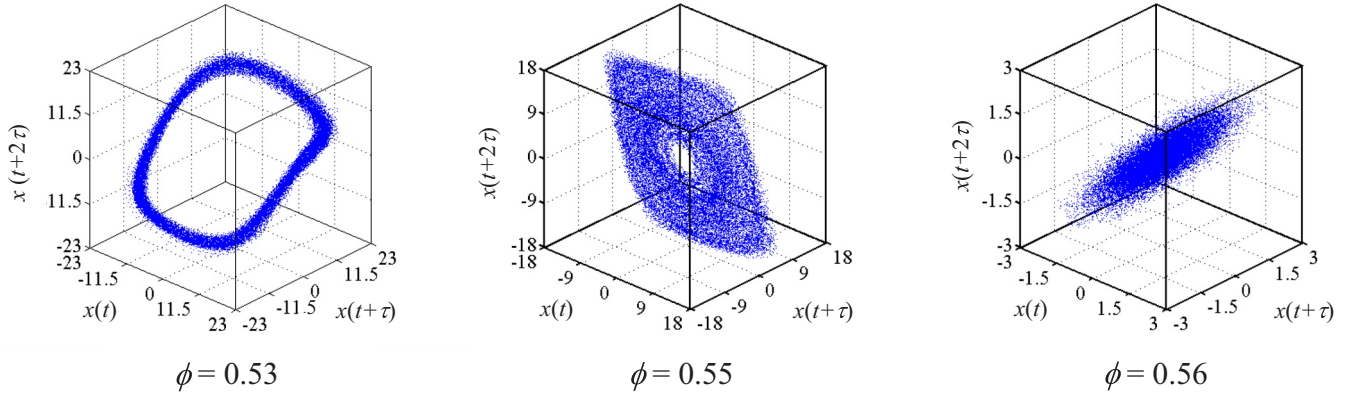


FIG. 2. (Color online) Three-dimensional phase space $(x(t), x(t + \tau), x(t + 2\tau))$ for different equivalence ratios ϕ . Thermoacoustic combustion oscillations at $\phi = 0.53$ exhibit a limit cycle with a relatively large width of periodic orbits. A torus-like structure with an increased width of the orbits appears at a higher equivalence ratio of $\phi = 0.55$. The attractor at $\phi = 0.56$ does not appear to exhibit the ordered structure during the degeneration process.

density distribution p_d of the nondimensional Euclidian distance $d_M (= \|\mathbf{x}_i - \mathbf{x}_j\| / \|\mathbf{x}_i - \mathbf{x}_j\|_{\max})$ between the pair \mathbf{x}_i and \mathbf{x}_j in three-dimensional phase space is shown in Fig. 3 for different ϕ , where $\|\mathbf{x}_i - \mathbf{x}_j\|_{\max}$ corresponds to the outer diameter of the attractor. We observe two notable peaks for thermoacoustic combustion oscillations at $\phi = 0.53$. They disappear at $\phi = 0.55$ and the shape of p_d plotted against d_M becomes semicircular. Upon increasing ϕ to 0.56, the distribution of p_d changes to one with a single distinct peak, which corresponds to the form represented by Eq. (8). Note

that the values of μ and σ^2 are 0.61 and 2.58, respectively:

$$p_d(100d_M|\mu, \sigma) = \frac{1}{\sqrt{2\pi\sigma^2}(100d_M)} \times \exp\left[\frac{-\{\ln(100d_M) - \mu\}^2}{2\sigma^2}\right]. \quad (8)$$

It is interesting to note that p_d has the logarithmic normal distribution. These results indicate that the probability density of nondimensional distances between the position vectors in the phase space is important for capturing the important dynamical changes in thermoacoustic combustion oscillations.

Figure 4 shows the spatial distribution of $\mathbf{R}_{i,j}$ for different ϕ . Note that it consists of 5000×5000 points in this study, corresponding to the temporal evolutions of p for $0 \text{ s} \leq t \leq 15 \text{ s}$. $\mathbf{R}_{i,j}$ at $\phi = 0.53$ is composed of regularly arrayed geometrical structures. These regular structures still persist for higher ϕ up to 0.55. However, $\mathbf{R}_{i,j}$ at $\phi = 0.56$ exhibits a homogeneous structure in a local region while retaining the regular structures, indicating the appearance of chaotic behavior in the combustion dynamics. As shown in Fig. 2, the torus-like structure in the phase space indicates the possible existence of quasiperiodic oscillations. It is well known that, although power spectrum analysis is classical and conventional, it is reliable for discussing the possible existence of quasiperiodic oscillations. We therefore examine the power spectrum density distribution of p at $\phi = 0.55$, which is shown in Fig. 5. The power spectrum density obtained clearly consists of many distinctive peaks, which are attributed to linear combinations of frequencies f_1 and f_2 (e.g., $2f_2 - f_1, 2f_1 - f_2, 3f_1 - 2f_2, 2f_1$). Note that f_1 corresponds to the 1/4 acoustic mode in the longitudinal direction of the combustor. The appearance of linear combinations of frequencies verifies the formation of quasiperiodic oscillations. These results show that thermoacoustic combustion oscillations bifurcate to quasiperiodic oscillations prior to the degeneration of the dynamics. Cartwright *et al.* [64] have shown the organization of three-frequency resonances in dynamical systems by generalizing the Farey tree structure of two-frequency systems to three frequencies. On this basis, we here consider a three-frequency system with two

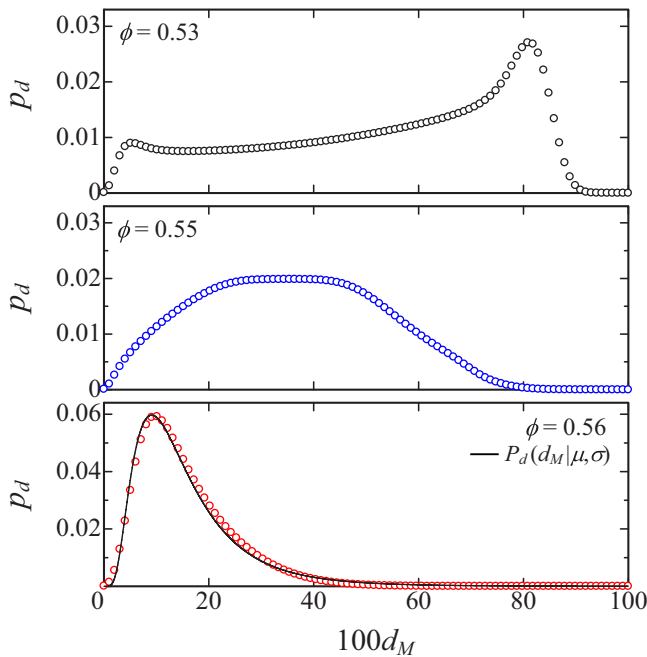


FIG. 3. (Color online) Probability density of the nondimensional Euclidian distance $d_M (= \|\mathbf{x}_i - \mathbf{x}_j\| / \|\mathbf{x}_i - \mathbf{x}_j\|_{\max})$ between \mathbf{x}_i and \mathbf{x}_j in three-dimensional phase space for different equivalence ratios ϕ . Two notable peaks of p_d appear for thermoacoustic combustion oscillations at $\phi = 0.53$. They disappear at $\phi = 0.55$ and the shape of p_d plotted against d_M becomes semicircular. The distribution of p_d changes to one with a single distinct peak at $\phi = 0.56$.

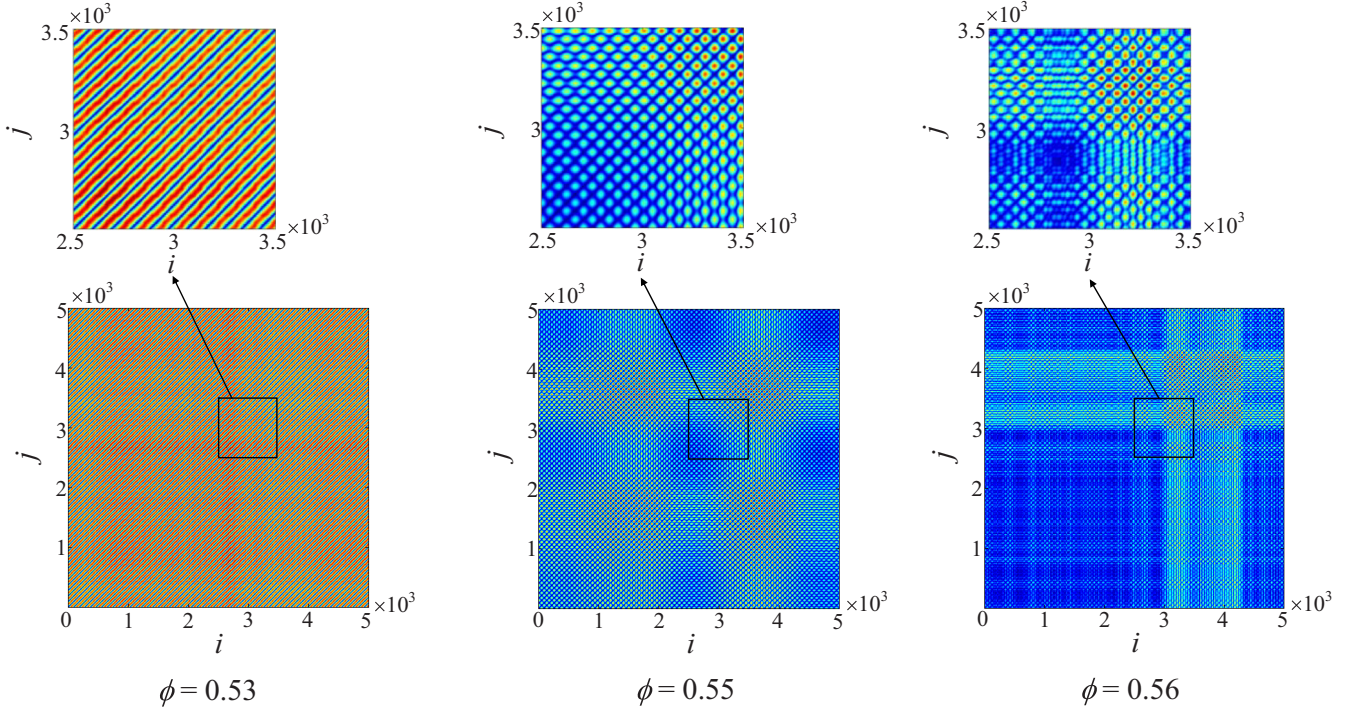


FIG. 4. (Color online) Spatial distribution of $\mathbf{R}_{i,j}$ for different equivalence ratios ϕ . $\mathbf{R}_{i,j}$ at $\phi = 0.53$ is composed of a regular array of geometrical structures. These regular structures still persist for higher ϕ up to 0.55. $\mathbf{R}_{i,j}$ at $\phi = 0.56$ exhibits a homogeneous structure in a local region while retaining the regular structures.

external frequencies, $f_a = 606$ Hz and $f_b = 896$ Hz, in the power spectrum. The rescaled frequencies \tilde{f}_a and \tilde{f}_b , respectively defined as $f_a/(f_a + f_b)$ and $f_b/(f_a + f_b)$, are obtained by continued-fraction expansion. The convergents of \tilde{f}_a and \tilde{f}_b are $1/2$, $2/5$, $23/57$, $140/347$, $303/751$ and $1/2$, $3/5$, $34/57$, $207/347$, $448/751$, respectively. The median frequencies \tilde{f}_s [$=(f_a + f_b)/(p_i + q_i)$, where $p_i + q_i$ is the denominator of the convergents] become $1502/2 = 751$ Hz, $1502/5 = 300.4$ Hz, $1502/57 = 26.35$ Hz, $1502/347 = 4.33$ Hz, and $1502/751 = 2$ Hz. \tilde{f}_s with the median frequency of 300.4 Hz nearly corresponds to the frequency f_1 at the peak in the spectrum. This indicates that three-frequency resonances are associated with the formation of quasiperiodic oscillations.

Figure 6 shows the variation in $\langle \text{Ind}_k \rangle$ in terms of $T_r \Delta t$ for the original time series of x at $\phi = 0.56$. $\langle \text{Ind}_k \rangle$ monotonically increases with increasing $T_r \Delta t$ for all D but exhibits small periodic fluctuations in the scaling region ranging from $T_r \Delta t = 3 \times 10^{-4}$ to 7×10^{-4} s. In our preliminary test, the periodic fluctuations remain nearly unchanged even under a broad range of k from 5 to 1000, where k is the number of \mathbf{x}_k . The presence of periodic fluctuations has been discussed by Kantz and Schreiber [20], but they are observable for chaotic oscillations in a different type of thermoacoustic combustion system [65] by using the algorithm of Kantz [35]. The histogram of λ obtained by the resampling method [50–52] at $\phi = 0.56$ is shown in Fig. 7. All λ exhibit positive values, and the distribution of λ is approximately Gaussian. Note that a similar distribution is obtained for different D . The peak value of λ , denoted by λ_p , is 1.14×10^{-2} (1/s). Variations in λ_p , the standard deviation of λ denoted by σ , and the 95% confidence

interval are shown in Table I for different D at $\phi = 0.56$. λ_p is positive for all D with 95% confidence, indicating the appearance of chaotic dynamics. When taking into account the use of nonlinear time series analysis in actual experiments, we encounter the problem that the noise inherently included in experimental data is inescapably superimposed on the pressure fluctuations. The presence of noise diminishes the accuracy of the estimated maximal Lyapunov exponent. It has been pointed out by Kantz and Schreiber [20] that a noise of a few percent results in the imperfect use of the algorithms adopted for nonlinear time series analysis. Because $\langle \text{Ind}_k \rangle$ slightly oscillates in the scaling region, the filtering out of noise [20] is required for our next study. The maximal Lyapunov exponents estimated by using a nonparametric neural network and their hypothesis tests enable us to detect chaos in a noisy system [66]. Such an analysis would also be of importance to more reliably show the presence of chaos in the degenerated combustion dynamics. It is well known that fractal dimension is an important indicator for discussing the possible presence of chaos from the viewpoint of geometrical structure. We adopted the well-known and standard correlation dimension method [33] for the pressure fluctuations at $\phi = 0.56$, but note that it is difficult to find a reliable scaling region to estimate the correlation dimension even for high-dimensional phase reconstruction.

Figure 8 shows the variation in the correlation coefficient C obtained from the local nonlinear predictor at $\phi = 0.56$ as a function of the prediction time t_p . As shown in Fig. 8(a), we can observe one-step-ahead prediction of x with relatively high accuracy (C is 0.95 at $t_p = 3.91 \times 10^{-5}$ s), and the manifestation of long-term unpredictability characteristics

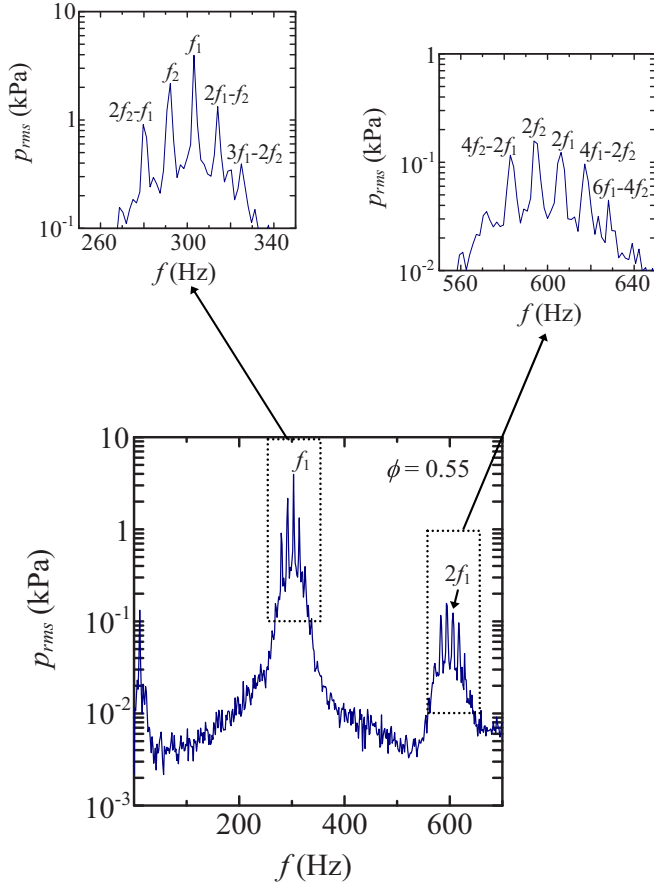


FIG. 5. (Color online) Power spectrum density distribution of p at equivalence ratio $\phi = 0.55$. The power spectrum density clearly consists of many distinctive peaks, which are attributed to linear combinations of frequencies f_1 and f_2 (e.g., $2f_2 - f_1$, $2f_1 - f_2$, $3f_1 - 2f_2$, $2f_1$).

when t_p exceeds approximately $t_p = 2.34 \times 10^{-4}$ s. A similar trend of C in terms of t_p is observed for the incremental process $\Delta x [=x(t_i + 1) - x(t_i)]$ [see Fig. 8(b)]. This is a clear signature of the emergence of chaotic dynamics. Note that we also obtain similar results for $\phi \geq 0.57$. Our results obtained by the local predictor and the estimations of the maximal Lyapunov exponent in combination with the resampling method [50–52] suggest that the degeneration of combustion dynamics at $\phi \geq 0.56$ is dominated by a chaotic process. The method of quantifying the short-term predictability and long-term unpredictability characteristics is schematically summarized in Fig. 9. If the combustion dynamics becomes complicated, the critical prediction time denoted as $t_{p,c}$ decreases and the gradient of the correlation coefficient $|d \ln C / d \ln t_p|$ increases with the prediction time. The predictability characteristics can be roughly evaluated by measuring these physical quantities. Variations in $t_{p,c}$ and $|d \ln C / d \ln t_p|$ with ϕ are shown in Fig. 10, which shows that they remain nearly unchanged for $0.52 \leq \phi \leq 0.54$. They abruptly change at $\phi = 0.56$ owing to the appearance of a chaotic process, then remain at a constant value up to $\phi = 0.60$. The significant changes in the short-term predictability and long-term unpredictability characteristics in terms of the equivalence ratio correspond

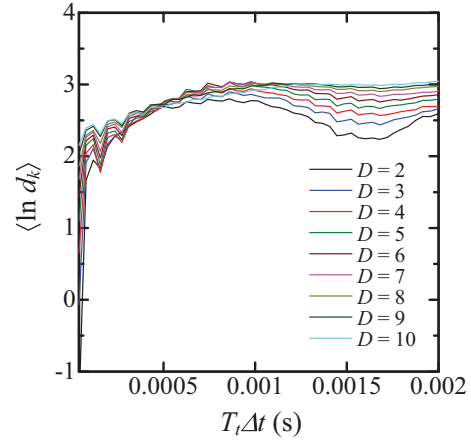


FIG. 6. (Color) Variation in $\langle \ln d_k \rangle$ in terms of $T_i \Delta t$ for the original time series of x at $\phi = 0.56$. $\langle \ln d_k \rangle$ monotonically increases with increasing $T_i \Delta t$ at all D .

closely to those obtained from the permutation entropy [67]. This clearly shows that both the method of quantifying the predictability characteristics and the method of distinguishing between deterministic chaos and stochastic dynamics using nonlinear forecasting methods are valid for characterizing complex combustion dynamics.

Figure 11 shows the variation in the multiscale entropy S_E as a function of the scaling factor s' for different ϕ . S_E at $\phi = 0.53$ exhibits gradual fluctuations with S_E close to zero around $s' = 94$. The complexity of p is lowest around $s' = 94$. We found that the ratio of the sampling frequency to the scaling factor, denoted as $\beta (=f_s/s'_m = 25600/94$; note that s'_m is the scaling factor at which S_E reaches zero), is nearly equal to the dominant frequency ($=276$ Hz) in the power spectrum density distribution. At a higher equivalence ratio of $\phi = 0.55$, s'_m shifts to a lower value, corresponding to the shift to a higher dominant frequency of 303 Hz in the power spectrum (see Fig. 5). This indicates that multiscale entropy enables us to extract the hidden regular dynamics in thermoacoustic combustion oscillations as an alternative to adopting power spectrum analysis. The appearance of quasiperiodicity causes

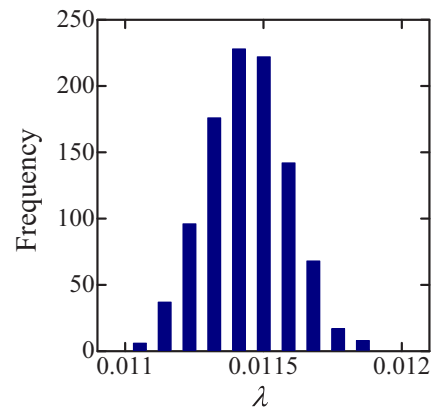


FIG. 7. (Color online) Histogram of λ obtained by the resampling method at $\phi = 0.56$. Its distribution is approximately Gaussian. The peak value of λ is 1.14×10^{-2} (1/s).

TABLE I. λ_p , σ , and the 95% confidence interval for different D at $\phi = 0.56$. λ_p is positive for all D with 95% confidence.

D	λ_p (1/s)	σ	[C.I. 95]
2	1.468×10^{-2}	1.68×10^{-4}	$[1.467 \times 10^{-2}, 1.469 \times 10^{-2}]$
3	1.302×10^{-2}	1.61×10^{-4}	$[1.301 \times 10^{-2}, 1.303 \times 10^{-2}]$
4	1.144×10^{-2}	1.48×10^{-4}	$[1.143 \times 10^{-2}, 1.145 \times 10^{-2}]$
5	9.722×10^{-3}	1.35×10^{-4}	$[9.715 \times 10^{-3}, 9.732 \times 10^{-3}]$
6	8.261×10^{-3}	1.33×10^{-4}	$[8.251 \times 10^{-3}, 8.267 \times 10^{-3}]$
7	6.658×10^{-3}	1.18×10^{-4}	$[6.649 \times 10^{-3}, 6.664 \times 10^{-3}]$
8	5.288×10^{-3}	1.04×10^{-4}	$[5.284 \times 10^{-3}, 5.297 \times 10^{-3}]$
9	4.107×10^{-3}	8.83×10^{-5}	$[4.101 \times 10^{-3}, 4.112 \times 10^{-3}]$
10	3.164×10^{-3}	7.29×10^{-5}	$[3.160 \times 10^{-3}, 3.169 \times 10^{-3}]$

S_E to increase at $\phi = 0.55$ in the entire range of s' compared with its value at $\phi = 0.53$. S_E at $\phi \geq 0.56$ is significantly increased by the degeneration of thermoacoustic combustion oscillations with quasiperiodicity. The interesting point to note here is that the degree of complexity gradually decreases with increasing scale factor, finally reaching the same degree as that of thermoacoustic combustion oscillations in the low-frequency region with $s' = 150$. We also observe that the complexity of the degenerated dynamics is dominated by the low-scaling-factor region, i.e., the high-frequency region. These results clearly demonstrate that a coarse-grained approach such as multiscale entropy is useful for quantifying the degree of complexity in combustion dynamics over a broad range of temporal scales. To the best of our knowledge, the applicability of the nonlinear time series analyses presented herein has not been explored in previous studies on combustion instability in gas-turbine model combustors.

More recently, the Indian Institute of Technology Madras group has carried out nonlinear time series analysis mainly involving the binary version of recurrence plots and the 0-1 test [68] for self-excited thermoacoustic combustion

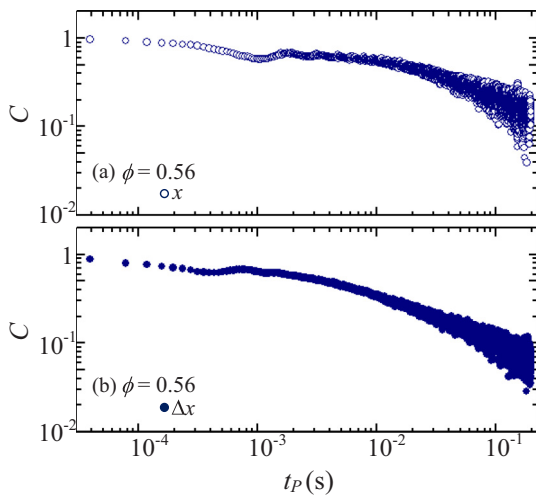


FIG. 8. (Color online) Variation in correlation coefficient C obtained by the local nonlinear predictor at $\phi = 0.56$ as a function of t_p . One-step-ahead prediction of x is achieved with relatively high accuracy (C is 0.95 at $t_p = 3.91 \times 10^{-5}$ s). In contrast, C for the incremental process Δx is about 0.89 at $t_p = 3.91 \times 10^{-5}$ s.

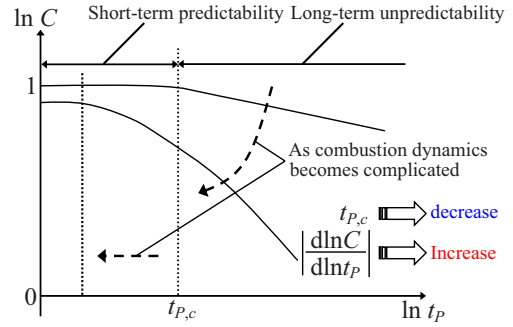


FIG. 9. (Color online) Method of quantifying short-term predictability and long-term unpredictability characteristics.

systems under turbulent flow conditions using different types of turbulent premixed combustors: swirled-stabilized-type and bluff-body-type combustors [69,70]. The University of Cambridge group has also considered the phase space and its Poincaré map for a swirled-stabilized turbulent premixed combustor subjected to acoustic forcing [71]. The quasiperiodicity [71], the synchronization of the self-excited mode with the forced mode [71], and intermittent bursts [69,70] were captured by nonlinear time series analysis in addition to conventional power spectrum analysis, providing new ideas for dealing with the physical mechanism behind thermoacoustic combustion instability. The findings obtained in previous studies [25–27] using ducted laminar premixed flames also show the applicability of nonlinear time series analysis to present-day combustion problems. In parallel with these works, our more recent studies [44,72] dealing with a laboratory-scale premixed gas-turbine model combustor under a nonpreheated mixture condition have set out a new methodology for distinguishing between deterministic and stochastic processes by extending the concept of the SM algorithm, which involves the update of the library data in phase space. They also include a proposed method of online early detection and a method of preventing lean blowout. Note that nonlinear invariants of pressure fluctuations in terms of the Reynolds number have been estimated by Nair *et al.* [69] with the aim of detecting the impending instability. The experimental

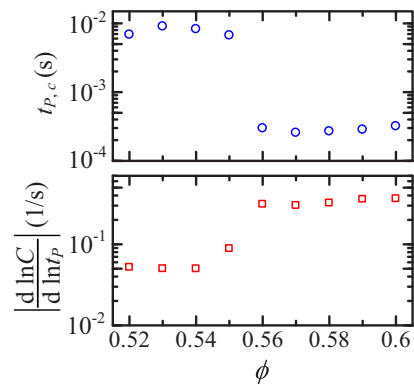


FIG. 10. (Color online) Variations in $t_{p,c}$ and $|d \ln C / d \ln t_p|$. $t_{p,c}$ and $|d \ln C / d \ln t_p|$ remain nearly unchanged for $0.52 \leq \phi \leq 0.54$. They abruptly change at $\phi = 0.56$ owing to the appearance of chaotic process, and then remain at a constant value up to $\phi = 0.60$.

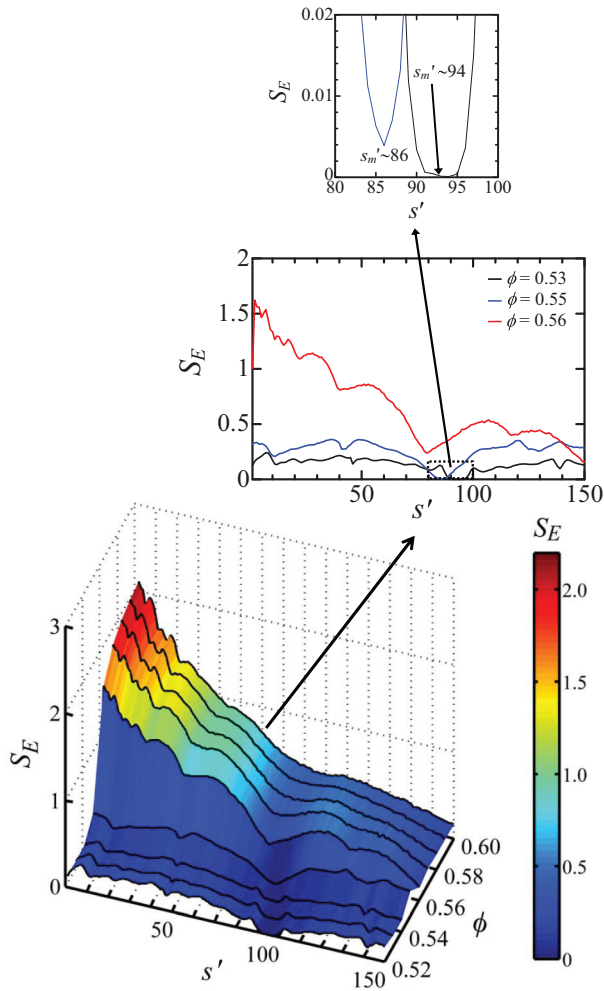


FIG. 11. (Color) Variation in multiscale entropy S_E as a function of scaling factor s' for different ϕ . S_E at $\phi = 0.53$ exhibits gradual fluctuations with S_E close to zero around $s' = 94$. s'_m , the scaling factor at which S_E reaches zero, shifts to a lower value at a higher equivalence ratio of $\phi = 0.55$. The appearance of quasiperiodicity causes S_E to increase at $\phi = 0.55$ in the entire range of s' compared with its value at $\phi = 0.53$. S_E at $\phi \geq 0.56$ is significantly increased by the degeneration of thermoacoustic combustion oscillations with quasiperiodicity.

and theoretical studies [44,69–72] reported thus far show that dynamical systems theory provides not only a fresh take on combustion instability but also a new methodology for controlling the combustion state in premixed-type turbulent combustors. Although our recent and earlier works, including the present one, globally interpret the dynamic behavior of thermoacoustic combustion instability as periodic oscillations, here we reveal in more detail the nature of the periodic oscillations by making use of a complex network approach [73]. This point is extensively discussed in Ref. [73]. Finally, the following three points should be taken into account in our next study:

(1) In a previous study by Tachibana *et al.* [55], the distribution of the peak fluctuation amplitude plotted against the axial location clearly showed that the self-excited instability mode was governed by a quarter-wave mode of the combustion

chamber in the longitudinal direction. The existence of this mode was observed for the transition process to the degenerated combustion dynamics. The effect of thermoacoustic coupling, measured by the local Rayleigh index, strongly appeared in the flame base about 10 mm downstream from the inlet of the combustion chamber [55]. In this study, we focused on investigating the dynamical properties of pressure fluctuations measured at this axial location, but the pressure fluctuations at different locations should also be analyzed in our next study to obtain a better understanding of the spatial effects on dynamical properties.

(2) Nair *et al.* [74] have recently investigated the short-term temporal evolution of Shannon entropy in recurrence structures during low- to high-amplitude oscillations for two types of thermoacoustic combustion system. To elucidate the relationship between the dynamical properties and the physical mechanisms of the observed combustion dynamics, in our next study it will be necessary to correlate the structural quantities such as the flame surface density with the dynamical properties for the short-term behavior of both pressure and heat release rate fluctuations, focusing on the transition process in the degenerated combustion process.

(3) There is an interesting question related to the utility of the nonlinear forecasting methodologies presented here. It has been reported by Nair *et al.* [69] that the method of Kaplan and Glass [75], known as a prototype of the Wayland test [41], which involves the null hypothesis method with the random shuffling of pressure fluctuations, suggests the possible presence of high-dimensional chaos in combustion noise. The presence of multifractality including the measure of the Hurst exponent also showed the possible existence of deterministic chaos [76]. How can one understand the dynamic behavior of combustion noise by using our methodologies? We need to examine this interesting issue in future studies to provide better methodologies for treating the nonlinearity in complex combustion dynamics.

V. CONCLUDING REMARKS

We characterized the dynamic behavior of combustion instability in a fundamentally and practically important gas-turbine combustion system, a lean premixed-type gas-turbine model combustor consisting of a swirl-stabilized turbulent flame under a preheated mixture condition, on the basis of dynamical systems theory. Our previous studies [39,40] have shown that the dynamic behavior of combustion instability in close proximity to lean blowout is dominated by a stochastic process that transits to periodic oscillations created by thermoacoustic combustion oscillations via chaos with increasing equivalence ratio. This study has focused on the emergence of the quasiperiodic and the subsequent aperiodic fluctuations with a further increase in the equivalence ratio. We incorporated a variety of nonlinear time series analyses not usually included in traditional combustion physics. These include the colored version of recurrence plots, the maximal Lyapunov exponent in combination with the resampling method [50–52], a nonlinear forecasting method: an extended version of the Sugihara–May (SM) algorithm [45] as a local predictor, and multiscale entropy. Thermoacoustic combustion oscillations exhibit a limit cycle with a relatively large width

of periodic orbits. An increase in the equivalence ratio leads to degenerated dynamics with a smaller attractor via the emergence of a torus-like structure. The power spectrum density for the torus-like structure has many distinctive peaks consisting mainly of linear combinations of frequencies. One of these peaks corresponds to the 1/4 acoustic mode in the longitudinal direction of the combustor, which clearly verifies the formation of quasiperiodic oscillations. The nonlinear forecasting methodology we proposed as an extended version of the SM algorithm, which involves the update of library data, has potential use for distinguishing between deterministic chaos and stochastic dynamics during the degeneration process in combustion instability. It gives us the interpretation that the degeneration of dynamics is dominated by a chaotic process. The multiscale entropy clearly shows that the complexity of the degenerated dynamics is dominated by a low-scaling-factor

region, i.e., a high-frequency region. On the basis of the findings obtained by the above analysis, we conclude that the dynamic behavior of thermoacoustic combustion oscillations undergoes a significant transition from periodic oscillations to chaotic fluctuations via quasiperiodic oscillations. The presented nonlinear time series analysis allows us to clarify the characteristics of complex combustion dynamics in a gas-turbine model combustor.

ACKNOWLEDGMENTS

H.G. was partially supported by a Grant-in-Aid for Young Scientists (A) from the Ministry of Education, Culture, Sports, Science and Technology of Japan (MEXT), the JGC-S Scholarship Foundation, and the Japan Gas Association Research Grant.

-
- [1] S. Candel, *Proc. Combust. Inst.* **29**, 1 (2002).
- [2] *Combustion Instabilities in Gas Turbine Engines: Operational Experience, Fundamental Mechanisms and Modeling*, edited by T. C. Lieuwen and V. Yang, Progress in Astronautics and Aeronautics, Vol. 210 (American Institute of Aeronautics and Astronautics, Reston, 2005).
- [3] K. Balasubramanian and R. I. Sujith, *Phys. Fluids* **20**, 044103 (2008).
- [4] T. Biwa, Y. Tashiro, U. Mizutani, M. Kozuka, and T. Yazaki, *Phys. Rev. E* **69**, 066304 (2004).
- [5] T. Biwa, Y. Tashiro, M. Ishigaki, Y. Ueda, and T. Yazaki, *J. Appl. Phys.* **101**, 064914 (2007).
- [6] T. Yoshida, T. Yazaki, H. Futaki, K. Hamaguchi, and T. Biwa, *Appl. Phys. Lett.* **95**, 044101 (2009).
- [7] T. Biwa, D. Hasegawa, and T. Yazaki, *Appl. Phys. Lett.* **97**, 034102 (2010).
- [8] H. Hatori, T. Biwa, and T. Yazaki, *J. Appl. Phys.* **111**, 074905 (2012).
- [9] *Lean Combustion, Technology and Control*, edited by D. Dunn-Rankin (Academic Press, London, 2008).
- [10] G. Searby and D. Rochwerger, *J. Fluid Mech.* **231**, 529 (1991).
- [11] V. Bychkov, *Phys. Fluids* **11**, 3168 (1998).
- [12] X. Wu, M. Wang, P. Moin, and N. Peters, *J. Fluid Mech.* **497**, 23 (2003).
- [13] C. J. Lawn and W. Polifke, *Combust. Sci. Technol.* **176**, 1359 (2004).
- [14] W. Polifke and C. J. Lawn, *Combust. Flame* **151**, 437 (2007).
- [15] V. Akkerman and C. K. Law, *Phys. Fluids* **25**, 013602 (2013).
- [16] J. Yáñez, M. Kuznetsov, and R. Redlinger, *Combust. Flame* **160**, 2009 (2013).
- [17] Y. Huang and V. Yang, *Prog. Energy Combust. Sci.* **35**, 293 (2009).
- [18] T. C. Lieuwen, *Unsteady Combustor Physics* (Cambridge University Press, Cambridge, 2012).
- [19] K. S. Chan and H. Tong, *Chaos: a Statistical Perspective* (Springer Verlag, Berlin, 2001).
- [20] H. Kantz and T. Schreiber, *Nonlinear Time Series Analysis*, 2nd ed. (Cambridge University Press, Cambridge, 2004).
- [21] M. Small, *Applied Nonlinear Time Series Analysis: Applications in Physics, Physiology and Finance* (World Scientific Publishing, Singapore, 2005).
- [22] C. S. Daw, J. F. Thomas, G. A. Richards, and L. L. Narayanaswami, *Chaos* **5**, 662 (1995).
- [23] S. Datta, S. Mondal, A. Mukhopadhyay, D. Sanyal, and S. Sen, *Combust. Theory Modell.* **13**, 17 (2009).
- [24] S. Mondal, A. Mukhopadhyay, and S. Sen, *Combust. Theory Modell.* **16**, 59 (2012).
- [25] L. Kabiraj, A. Saurabh, P. Wahi, and R. I. Sujith, *Chaos* **22**, 023129 (2012).
- [26] K. Kashinath, Ph.D. thesis, University of Cambridge, 2013 (unpublished).
- [27] K. Kashinath, I. C. Waugh, and M. P. Juniper, *J. Fluid Mech.* **761**, 399 (2014).
- [28] T. Lieuwen, *J. Propul. Power* **18**, 61 (2002).
- [29] S. Kadowaki and N. Ohkura, *Trans. Jpn. Soc. Aeronaut. Space Sci.* **51**, 133 (2009).
- [30] H. Gotoda and T. Ueda, *Proc. Combust. Inst.* **29**, 1503 (2002).
- [31] L. K. B. Li and M. P. Juniper, *Proc. Combust. Inst.* **34**, 947 (2013).
- [32] H. Gotoda, T. Ikawa, K. Maki, and T. Miyano, *Chaos* **22**, 033106 (2012).
- [33] P. Grassberger and I. Procaccia, *Phys. Rev. Lett.* **50**, 346 (1983).
- [34] M. T. Rosenstein, J. J. Collins, and C. J. D. Luca, *Phys. D* **65**, 117 (1993).
- [35] H. Kantz, *Phys. Lett. A* **185**, 77 (1993).
- [36] J. Eckmann, S. O. Kamphorst, and D. Ruelle, *Europhys. Lett.* **4**, 973 (1987).
- [37] L. Kabiraj and R. I. Sujith, *J. Fluid Mech.* **713**, 376 (2012).
- [38] V. Nair and R. I. Sujith, *Chaos* **23**, 033136 (2013).
- [39] H. Gotoda, H. Nikimoto, T. Miyano, and S. Tachibana, *Chaos* **21**, 013124 (2011).
- [40] H. Gotoda, M. Amano, T. Miyano, T. Ikawa, K. Maki, and S. Tachibana, *Chaos* **22**, 043128 (2012).
- [41] R. Wayland, D. Bromley, D. Pickett, and A. Passamante, *Phys. Rev. Lett.* **70**, 580 (1993).
- [42] C. Bandt and B. Pompe, *Phys. Rev. Lett.* **88**, 174102 (2002).

- [43] E. Ott, *Chaos in Dynamical Systems*, 2nd ed. (Cambridge University Press, Cambridge, 2002).
- [44] H. Gotoda, Y. Shinoda, M. Kobayashi, Y. Okuno, and S. Tachibana, *Phys. Rev. E* **89**, 022910 (2014).
- [45] G. Sugihara and R. M. May, *Nature (London)* **344**, 734 (1990).
- [46] N. Cazelles and R. Ferriere, *Nature (London)* **355**, 25 (1992).
- [47] A. A. Tsonis and J. B. Elsner, *Nature (London)* **358**, 217 (1992).
- [48] Q. Yao and H. Tong, *Phys. D* **115**, 49 (1998).
- [49] H. Gotoda, M. Pradas, and S. Kalliadasis, *Int. J. Bifurcation Chaos Appl. Sci. Eng.* **25**, 1530015 (2015).
- [50] S. Giannerini and R. Rosa, *Phys. D* **155**, 101 (2001).
- [51] S. Giannerini and R. Rosa, *Studies in Nonlinear Dynamics and Econometrics* **8**, 1558 (2004).
- [52] S. Giannerini, R. Rosa, and E. L. Gonzalez, *Int. J. Bifurcation Chaos Appl. Sci. Eng.* **17**, 169 (2007).
- [53] J. S. Richman and J. R. Moorman, *Am. J. Physiol.-Heart Circ. Physiol.* **278**, H2039 (2000).
- [54] M. Costa, A. L. Goldberger, and C.-K. Peng, *Phys. Rev. Lett.* **89**, 068102 (2002).
- [55] S. Tachibana, L. Zimmer, Y. Kurosawa, and K. Suzuki, *Proc. Combust Inst* **31**, 3225 (2007).
- [56] F. Takens, *Dynamical Systems of Turbulence*, Lecture Notes in Mathematics, Vol. 898 (Springer-Verlag, Berlin, 1981).
- [57] M. B. Kennel, R. Brown, and H. D. I. Abarbanel, *Phys. Rev. A* **45**, 3403 (1992).
- [58] A. M. Fraser and H. L. Swinney, *Phys. Rev. A* **33**, 1134 (1986).
- [59] A. C. Davison and D. V. Hinkley, *Bootstrap Methods and Their Application* (Cambridge University Press, Cambridge, 1997).
- [60] R. Davidson and J. G. Mackinnon, Bootstrap Tests: How Many Bootstraps, Queen's Economics Department Working Paper **1036** (2001).
- [61] S. M. Pincus, *Proc. Natl. Acad. Sci. USA* **88**, 2297 (1991).
- [62] M. Costa, A. L. Goldberger, and C. K. Peng, *Phys. Rev. E* **71**, 021906 (2005).
- [63] Y. Huang and V. Yang, *Combust. Flame* **136**, 383 (2004).
- [64] J. H. E. Cartwright, D. L. Gonzalez, and O. Piro, *Phys. Rev. E* **59**, 2902 (1999).
- [65] L. Kabiraj, A. Saurabh, N. Karimi, A. Sailor, E. Mastorakos, A. P. Dowling, and C. O. Paschereit, *Chaos* **25**, 023101 (2015).
- [66] M. Shintani and O. Linton, *J. Econom.* **120**, 1 (2004).
- [67] K. Hayashi, H. Gotoda, Y. Okuno, and S. Tachibana, Proc. 52nd National Heat Transfer Symposium of Japan, J122 (2015) (in Japanese).
- [68] G. A. Gottwald and I. Melbourne, *Proc. R. Soc. London, Ser. A* **460**, 603 (2003).
- [69] V. Nair, G. Thampi, S. Karuppusamy, S. Gopalan, and R. I. Sujith, *Int. J. Spray Combust. Dyn.* **5**, 273 (2013).
- [70] V. Nair and R. I. Sujith, *Proc. Combust. Inst.* **35**, 3139 (2015).
- [71] S. Balusamy, L. K. B. Li, Z. Han, M. P. Juniper, and S. Hochgreb, *Proc. Combust. Inst.* **35**, 3229 (2015).
- [72] S. Domen, H. Gotoda, T. Kuriyama, Y. Okuno, and S. Tachibana, *Proc. Combust. Inst.* **35**, 3245 (2015).
- [73] Y. Okuno, M. Small, and H. Gotoda, *Chaos* **25**, 043107 (2015).
- [74] V. Nair, G. Thampi, and R. I. Sujith, *J. Fluid Mech.* **756**, 470 (2015).
- [75] D. T. Kaplan and L. Glass, *Phys. D* **64**, 431 (1993).
- [76] V. Nair and R. I. Sujith, *J. Fluid Mech.* **747**, 635 (2014).